

Vertical-orbital band center as an activity descriptor for hydrogen evolution reaction on single-atom-anchored 2D catalysts

Wen Qiao¹, Shiming Yan^{1*}, Deyou Jin¹, Xiaoyong Xu², Wenbo Mi³, Dunhui Wang¹

1 School of Electronics and Information, Hangzhou Dianzi University, Hangzhou 310018, China

2 School of Physics Science and Technology, Yangzhou University, Yangzhou, 225002, China

3 Tianjin Key Laboratory of Low Dimensional Materials Physics and Preparation Technology, School of Science, Tianjin University, Tianjin 300354, China

ABSTRACT:

The d-band center descriptor based on the adsorption strength of adsorbate has been widely used in understanding and predicting the catalytic activity in various metal catalysts. However, its applicability is unsure for the single-atom-anchored two-dimensional (2D) catalysts. Here, taking the hydrogen (H) adsorption on the single-atom-anchored 2D basal plane as example, we examine the influence of orbitals interaction on the bond strength of hydrogen adsorption. We find that the adsorption of H is formed mainly via the hybridization between the 1s orbital of H and the vertical d_{z^2} orbital of anchored atoms. The other four projected d orbitals ($d_{xy}/d_{x^2-y^2}$, d_{xz}/d_{yz}) have no contribution to the H chemical bond. There is an explicit linear relation between the d_{z^2} -band center and the H bond strength. The d_{z^2} -band center is proposed as an activity descriptor for hydrogen evolution reaction (HER). We demonstrate that the d_{z^2} -band center is valid for the single-atom active sites on a single facet, such as the basal plane of 2D nanosheets. For the surface with multiple facets, such as the surface of three-dimensional (3D) polyhedral nanoparticles, the d-band center is more suitable.

* Corresponding author: shimingyan@hdu.edu.cn

1. Introduction

As a high-density, pollution-free green energy, hydrogen energy is expected to become one of pillar of energy source in the future. Production of hydrogen via electrochemical water splitting is an important way to obtain hydrogen energy, and received greatly attention over the past few decades.[1-4] Finding efficient and inexpensive HER electrocatalyst is the key for the large-scale implementation of water electrolysis technologies.[5-12]

MoS₂ is a kind of high-efficiency and cheap 2D transition-metal sulfide (TMD) electrocatalytic material for HER.[13-23] It is considered to be a potential replacement for Pt-based noble metal catalysts. However, its activity is mainly derived from the unsaturated S atoms at the edges, which limit the further enhancement of the HER catalytic activity due to the low atom proportion of the edges. The basal plane with high atom proportion and high exposed area is inert.[23-25] How to add active sites onto the basal plane is one of research subject for such materials in the electrochemical HER. One strategy is to anchor single transition-metal atoms (TMs) on the basal planes. Up to now, many experiment studies have reported highly stable and highly active single-atom-anchored 2D catalyst.[15, 18, 19, 26-30] However, there are few reports associated with the essential mechanism of the activity from the perspective of electronic structure in this new system. Essentially understanding the mechanism of the activity can present rational guiding for the design of high-efficiency catalysts by selecting, high-abundance, low-cost metal atoms and 2D supports as building blocks.

The process of electrocatalytic HER consists of two steps.[31] The first step is the Volmer reaction. In acid media, this step is a process of recombination of electrons and protons. Electrons are transferred to active sites on the catalyst surface and coupled with protons in the solution to generate adsorbed H atoms. The second step is the desorption reaction. This process has two paths, namely the Heyrovsky reaction (the adsorbed H atom and another proton in the solution combine to form H molecule through secondary electron transfer) and the Tafel reaction (two adsorbed H atoms combine to produce H molecule). From the perspective of the entire reaction process, there are two possible paths for the HER, namely Volmer-Heyrovsky and Volmer-Tafel paths. Nevertheless, whichever path, the entire reaction all undergoes the process of H adsorption and desorption. The reaction intermediates of the two paths are all the adsorbed H atoms. It has been

verified that an ideal HER electrocatalyst must be facilitated to both H adsorption and desorption.[32, 33] The Gibbs free energy of H adsorption is required to be close to zero, which means that the adsorption strength should be neither too strong nor too weak.[31, 34, 35] So how to control the adsorption strength of H on catalyst is one of the critical parameters in improving the catalytic activity for HER.

D-band center model can well describe the adsorption strength of the adsorbate on metals and their alloys and compounds, particularly in the case of the electronic structure changes under different conditions.[31, 34-38] In terms of this model, trends in the interaction energy between the adsorbate and the metal surface are governed by the coupling to the metal d bands, since the coupling to the metal sp states is essentially the same for the transition and noble metals.[31, 34, 38, 39] The adsorption strength is primarily determined by the energy band position of the d orbital, which is measured by the d-band center. As the d-band center rises, less electrons is filled in d bands, and stronger bond between the metal and adsorbate will be formed. The d-band center descriptor has been widely used to estimate the catalytic activity in various metal alloy catalysts, and given a well guide in the design of high-efficiency catalysts.[36, 37, 40]

However, for the single-atoms active sites on 2D basal planes, not all the d orbitals are effectively hybridized with the H 1s orbital. We know that the d orbital can be subdivided into five projected orbitals d_{xy} , $d_{x^2-y^2}$, d_{xz} , d_{yz} , and d_{z^2} . These orbitals have different spatial symmetry and different energy level under the effects of the ligand field. On the 2D basal planes, due to the different symmetry and energy level, these projected d orbitals have different degrees of interaction with the H 1s orbital and thus have different contributions to the binding energy of H adsorption. So the accurate description of HER activity based on the H adsorption energy requires paying more attention to the electronic structure characteristics of the projected d orbitals.

Gibbs free energy calculated by density functional theory (DFT) has been widely used as the reactive descriptor in heterogeneous catalysis. The description of HER activity of single-atom active sites on 2D basal plane also mainly employs this parameter.[16, 18, 22, 41-43] However, this descriptor could not essentially understand the origin of the catalytic activity from the intrinsic features of the catalyst. There are few reports on the mechanism of the activity origin for the single-atom active sites, but the analysis is only based on the energy level of the total d-orbital band.[18, 22, 41] As above mentioned, parts of the projected d orbitals, especially the in-plane

projected d orbitals, d_{xy} and $d_{x^2-y^2}$, are completely inert due to the unique structure of the 2D basal-plane systems. Thus the employing of the total d-orbital band to explore the mechanism in the new system might be sketchy. Up to now, no research focuses on the dependence of features of the projected d orbitals on the activity for the single-atom active sites on 2D basal plane.

Herein, we improve the d-band model and enable it to be more applicable for the single-atom-anchored 2D basal plane system in HER activity. The metallic 1T phase of MoS_2 (1T- MoS_2) was chosen as the 2D basal-plane substrate. Various TMs were selected to anchor on the basal plane. Using first-principles calculations based on DFT, the interaction between H 1s orbital and the projected d orbitals of the anchored TMs was examined. It is found that the binding of H and the single-atom active sites on basal plane is formed mainly via the hybridization of H 1s orbital and the vertical d_{z^2} orbital of the anchored TMs. There is an obvious relationship between the d_{z^2} -band center and the H bond strength. A descriptor based on the d_{z^2} -band center is proposed to estimate the electrocatalytic activity of HER. The similarities and differences for the d-band center model and the d_{z^2} -band center model were discussed. The d_{z^2} -band center model is the further developing of d-band center model. But they are adapted for different systems. The d_{z^2} -band center is only valid for the 2D basal plane system, while the d-band center is more suitable for the surface of polyhedral nanoparticles system.

2. Methods

We carried the calculations of the energy and electronic structure for all the systems involved using the VASP code. Calculations were performed (with a plane wave basis code) within the generalized gradient approximation, following Perdew-Burke-Ernzerhof (GGA-PBE) for the exchange-correlation function. The plane-wave energy cut-off is 450 eV and an energy convergence threshold is 10^{-6} eV. The Monkhorst-Pack k-point mesh of $7 \times 7 \times 1$ was set as the Brillouin-zone integration. All of the TMs anchoring on MoS_2 systems were modeled by a supercell of lateral size (2×2) and a vacuum region of 15 Å is used to decouple the periodic images.

The H adsorption energy is estimated as [31]

$$\Delta E_{\text{H}} = E_{2\text{D-BP-SA}+\text{H}} - E_{2\text{D-BP-SA}} - \frac{1}{2}E_{\text{H}_2}$$

where $E_{2\text{D-BP-SA}}$ is the total energy for the systems of the TMs-anchored 2D basal plane of 1T- MoS_2 , $E_{2\text{D-BP-SA}+\text{H}}$ is the total energy for these systems with adsorbed H atoms, and the E_{H_2} is the energy for a hydrogen molecule in the gas phase.

The H₂ molecule adsorption energy is defined as

$$\Delta E_H = E_{2D-BP-SA+H_2} - E_{2D-BP-SA} - E_{H_2}$$

The d_{z²}-band center is calculated with the formula

$$d_{z^2} - center = \frac{\int E \rho_{d_{z^2}} dE}{\int \rho_{d_{z^2}} dE}$$

where, the $\rho_{d_{z^2}}$ is the PDOS of the d_{z²} orbital of the TMs at E energy.

The calculation of binding energy is done according to the following formula

$$E_{BE} = E_{2D-BP+TM} - E_{2D-BP} - E_{TM}$$

where E_{2D-BP} is the energy of 2D 1T-MoS₂ basal plane without anchored TMs, $E_{2D-BP+TM}$ is the energy of 2D 1T-MoS₂ basal plane with anchored TMs, E_{TM} is the energy of the TMs.

3. Results and discussion

The representative system with Co-anchored basal plane of 1T-MoS₂ (1T-MoS₂-Co) was chosen to examine the feature of H adsorption. On the basal plane of the 1T-MoS₂, there are three possible Co-anchored sites, Mo atop site, S atop site and hollow site (as shown in Figure S1). Previous experimental and theoretical studies have shown that the Co atom prefers to bond on the Mo atop sites.[15, 18, 19, 44] Here, the calculated binding energy for Co anchoring also indicates that the Mo atop site is the most stable sites for Co atom (Table S1). This can be ascribed to the extra Mo-Co bonding on the Mo atop site. It is noted that the similar results, due to the same reason, were also found in Fe, Co, Os, Ni anchored 2H phase of MoS₂. [26, 29, 45, 46]

For the H adsorption, we consider six kinds of positions (as shown in Figure S1, denoted as numbers) as the initial adsorbed position. After geometric optimization, the six initial geometric configurations all eventually evolve into that with H sitting on the Co atop site (Figure 1a). This suggests that, (1) compared to the S atom, the Co atom is the most attractive atom for H atom; (2) at the Co atop site, the H atom has the most efficiency attractive interaction with Co atom. As discussed below, these results can be attributed to the strong interaction between the unfilled vertical d_{z²} orbital of Co and the 1s orbital of H.

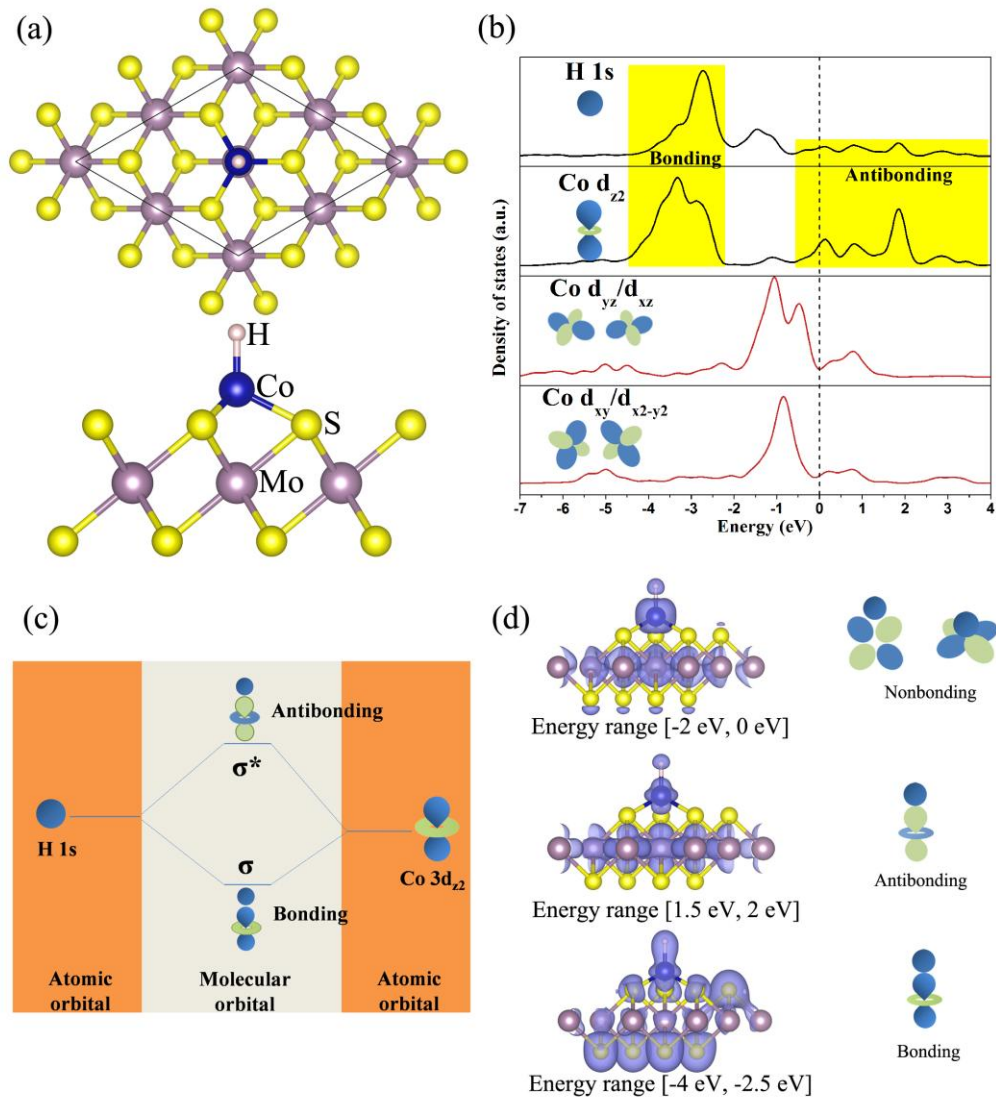


Figure 1. (a) Top and side view of H adsorbed supercell 1T-MoS₂-Co after geometric optimization. (b) PDOS of the H 1s, Co d_{xy}/d_{x²-y²}, Co d_{xz}/d_{yz} and Co d_{z²} orbitals for the H-adsorbed 1T-MoS₂-Co. (c) Schematic of interaction between H 1s and Co 3d_{z²} orbitals in terms of molecular orbital theory. (d) Charge density of the H-adsorbed 1T-MoS₂-Co at different energy range. Right is the schematic illustrations of the corresponding orbitals interaction.

Figure 1b gives the projected density of state (PDOS) of the H 1s, Co d_{xy}/d_{x²-y²}, Co d_{xz}/d_{yz} and Co d_{z²} orbitals for the H-adsorbed 1T-MoS₂-Co after geometric optimization. We can see that H 1s orbital profoundly hybridizes with the vertical d_{z²} orbital of the Co atom. Their bonding states locate at the energy range from -4 eV to -2.5 eV. For the corresponding antibonding states, besides a small part below the Fermi energy level, most of them distribute above the Fermi energy level. The interaction between the Co d_{z²} orbital and the H 1s orbital can be understood in terms of molecular orbital theory. As shown in Figure 1c, due to the symmetry matching, along the perpendicular direction of the basal plane, the H 1s orbital overlaps in phase with Co d_{z²} orbital to

form σ bonding state at low energy level, and overlaps out of phase to form σ^* antibonding state at high energy level. In order to more visibly identify the bonding between H 1s and Co d_{z^2} orbitals, we calculated the distribution of charge density of the H-adsorbed 1T-MoS₂-Co at different energy range. As shown in Figure 1d, at the energy range from -4 eV to -2.5 eV, where the Co d_{z^2} PDOS and H 1s PDOS appear resonance, electrons exhibit integration state at the middle position of H and Co, indicating the bonding state. At the energy range from 1.5 eV to 2 eV, an obvious node lies at the middle position of H and Co, suggesting the antibonding state. At the energy range from -2 eV to 0 eV, where the PDOS of Co is mainly occupied by the d_{xz}/d_{yz} and $d_{x^2-y^2}/d_{xy}$ orbitals, electrons distribute separately on they own atoms by oneself, meaning no bonding between them. The schematic illustrations of the corresponding orbitals interaction are shown in the right of Figure 1d. For the Co d_{xz}/d_{yz} and $d_{x^2-y^2}/d_{xy}$ orbitals, the H1s orbital overlap simultaneously with their positive phase and negative phase electron clouds. As a result, no bond is formed.

The hybridization between Co d_{z^2} and H 1s orbitals can be identified in the orbital-resolved bands structure. As shown in Figure S2, $d_{x^2-y^2}/d_{xy}$ bands completely separate from the H 1s orbital bands, indicating no coupling between them; for the d_{xz}/d_{yz} orbitals, there is only a few bands have slightly overlap with the H 1s orbital bands; However, for the d_{z^2} orbital, most of its bands profoundly hybridization with the H 1s orbital bands, suggesting their effective bonding.

To further confirm the interaction between Co d_{z^2} and H 1s orbitals, we set different distance of Co and H (Co-H) (Figure 2a), and calculated the corresponding PDOS. Decreasing the distance of Co-H will enlarge the overlap and induce high hybridization between Co d_{z^2} and H1s orbitals. We can speculate that, according to the molecular orbital theory, this will amplify the energy splitting of the bonding and antibonding states. Figure 2b shows the calculated PDOS. We can see that at large Co-H distance of 4.590 Å, the feature of Co d_{z^2} PDOS is almost the same as that without H adsorption (Figure 3a), indicating no interaction between the Co and H at this distance. As the Co-H distance decreases to 2.470 Å, the Co d_{z^2} and H 1s orbitals begin to hybridize. The PDOS of H 1s orbital appears downshift and resonance with the PDOS of Co d_{z^2} orbital. With further decreasing the distance, the resonance strength become stronger, the bonding state shift to lower energy level, and its energy difference compared to the antibonding state become more and more large. Different from the vertical d_{z^2} orbital, there is no changes for the PDOS of $d_{xy}/d_{x^2-y^2}$ and d_{xz}/d_{yz} orbitals with decreasing Co-H distance (Figure S3). These results further suggest that H

1s orbital only hybridizes with the vertical d_{z^2} orbital at the basal plane. For the nonvertical orbitals, $d_{xy}/d_{x^2-y^2}$ and d_{xz}/d_{yz} , the H 1s orbital has no bonding with them.

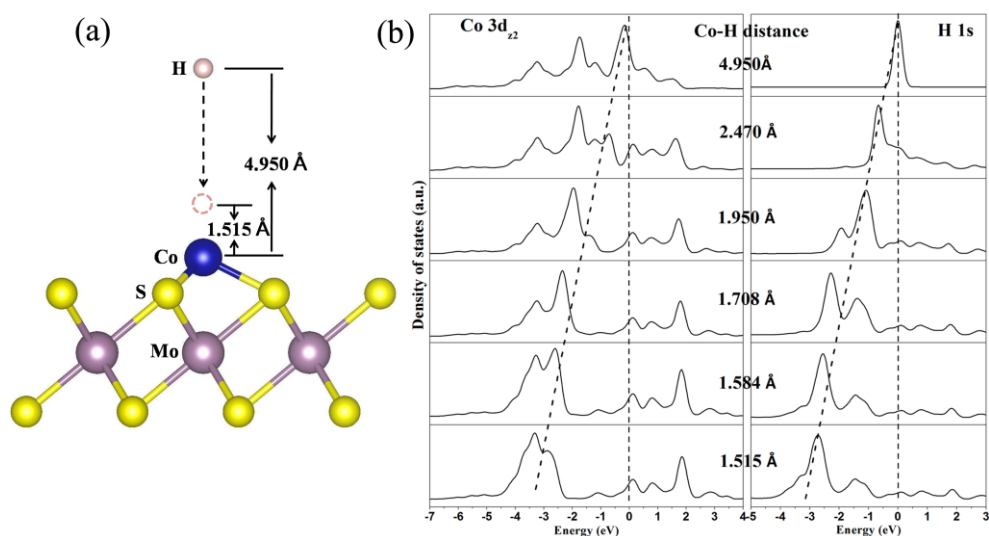


Figure 2. (a) Schematic for altering the Co-H distance. (b) PDOS of Co $3d_{z^2}$ and H 1s orbitals at different distance of Co-H.

Various factors of electric structure can influence the H adsorption energy on catalysis, such as the local d-band density of states at the Fermi level, the number of holes in the d bands, the width and shape of the d bands.[39] However, these factors usually could not measure the adsorption energy solely or are generally smaller corrections.[38] The d-band center has been verified to give a primary contribution towards the surface adsorption reactive of metals.[34-36, 38] For the 2D basal plane systems, since the chemical bond of H forms mainly through the interaction of the vertical d_{z^2} orbital, the band center of d_{z^2} orbital could play a primary role in determining the H adsorption energy. In order to confirm this, we calculated the PDOS of d_{z^2} of different 3d TMs anchored on the basal plane of 1T-MoS₂, and examined the correlation between the d_{z^2} -band center and H adsorption energy.

Similar to the Co anchoring, compared to the hollow site and S atop site, other 3d TMs also prefer to bond on the Mo atop site (Table S). So here we select this geometric configuration as the object to study the influence of d_{z^2} -orbital electronic structure on the strength of H adsorption. Figure 3a shows the d_{z^2} PDOS of the series anchored 3d TMs. The d_{z^2} -band center calculated from the d_{z^2} PDOS is shown in Figure 3b. The calculated H adsorption energy on the series 3d TMs is shown in the Figure 3c. We can see that, for the left atoms of the first row TM elements in the periodic table, the d_{z^2} -band centers locate at high energy level; while, at right of the periodic table,

the d_{z^2} -band centers of the 3d TMs locate at low energy level. From right Ni to left V, the d_{z^2} -band center shifts up gradually to high energy (Figure 3b). This relation can be attributed to the difference of the 3d orbital filling in the series 3d TMs. For the first row TM elements, the filling of 3d orbital gradually increase from left to right in the periodic table. Increasing the filling of 3d orbital will result in the reduction of the band center. Because the more filling means that more electrons occupy the states below Fermi level. As a consequence, the band center will be low away from Fermi level.

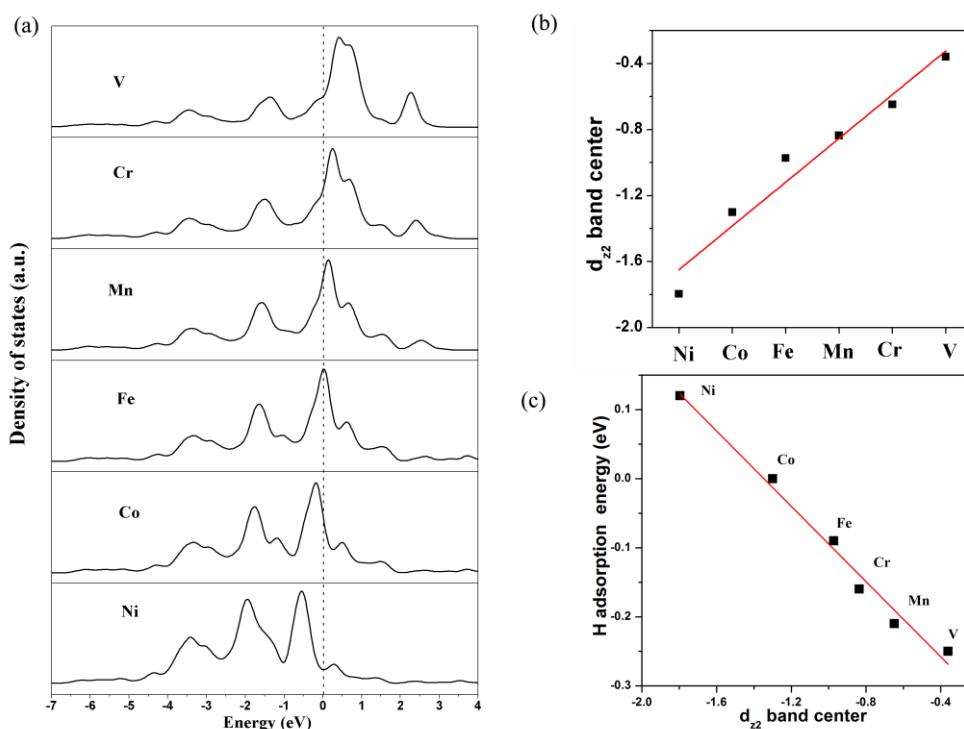


Figure 3. (a) PDOS of d_{z^2} for the series anchored 3d TMs on 1T-MoS₂. (b) Calculated d_{z^2} -band center for the series 3d TMs on basal planes of 1T-MoS₂. (c) The d_{z^2} -band center dependence of H adsorption energy for the series 3d TMs anchored on basal planes of 1T-MoS₂.

Figure 3c shows the d_{z^2} -band center dependence of H adsorption energy. There is obvious correlation between them. With increase of the d_{z^2} -band center, the H adsorption energy decreases approximately linearly. This relationship is the result of the different electron filling of the antibonding state formed by the hybridization with H. It is known that the bond strength is determined by the filling of the antibonding state.[34, 35] The more the empty antibonding state is, the higher the strength of bond is. Since the antibonding states are always above the d_{z^2} states, increase of d_{z^2} -band center will result in the rise of the antibonding state. Our calculated PDOS of the TMs with H adsorbed indeed show the upshift of the antibonding state with increase of the

d_{z^2} -band center (Figure S4). Therefore, increasing d_{z^2} -band center will lead to the strong H bond strength and low H adsorption energy.

Besides the filling of orbital, another way to change the position of d-band center is the strain. Strain has large influence on the width of d bands, but negligible influence on the d orbital filling. This will fix the d band to the Fermi level. With adding strain, system will have to compensate for variations in the width by shifting the d states up or down in energy.[35, 36] In order to further confirm the correlation between the d_{z^2} -band center and H adsorption energy, we added different strain to the typical system 1T-MoS₂-Co, and calculated the PDOS and H adsorption energy. The properties, in particular the energy, associated with d_{z^2} orbital are sensitive to the perpendicular strain. As the orientation of the d_{z^2} orbital is perpendicular to the basal plane, strain along this direction will significantly influence the overlap of the d_{z^2} orbital with others. Therefore, here we select to add the strain along the c axis, instead of a or b axis.

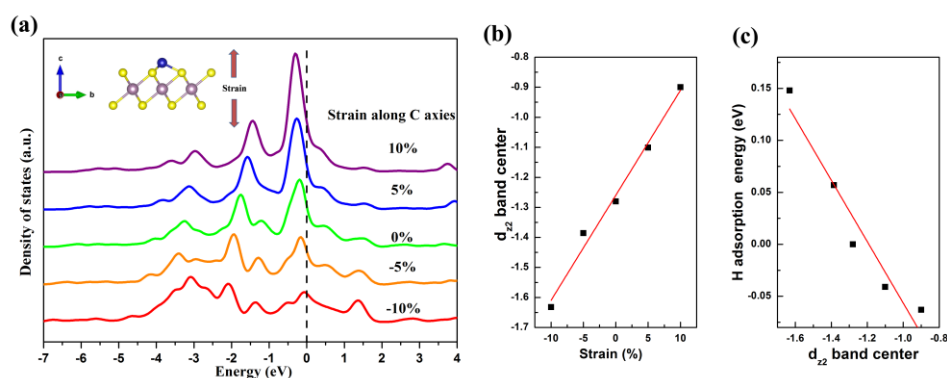


Figure 4. (a) PDOS of d_{z^2} orbital under different perpendicular strains for the 1T-MoS₂-Co. (b) The strain dependence of d_{z^2} -band center for the 1T-MoS₂-Co. (c) The d_{z^2} -band center dependence of H adsorption energy for the 1T-MoS₂-Co.

Figure 4a gives the PDOS of d_{z^2} orbital under different perpendicular strains for the 1T-MoS₂-Co. We can see that the tensile strain results in the band narrowing, and simultaneously the PDOS below Fermi level shift up to higher energy; while the compression strain leads to the change on the contrary. The calculated d_{z^2} -band center show proportionally dependence with variation of strain (Figure 4b). As is expected, the H adsorption energy also shows proportionally relationship with strain. Tensile strain reduces the H adsorption energy; compression strain enhances the H adsorption energy. The correlation between the H adsorption energy and the d_{z^2} -band center was plotted in Figure 4c. Obviously, with increasing the band center, the H

adsorption energy decrease linearly. This further confirms the influence of d_{z^2} -band center on the H bond strength.

In addition, we also calculated the adsorption energy of H_2 molecule on different 3d TM atoms anchored on 1T-MoS₂ (shown in Figure S6). For each 3d TM, the adsorption energy of H_2 molecule is larger than the H adsorption energy, indicating that H_2 molecule is unstable on the TM atoms compared to the adsorbed H. The forming H_2 molecule is easy to desorb from the TM atoms, and do not influence the adsorption of H atom. From the Figure S6, we can see that, similar to the H adsorption, H_2 molecule adsorption energy also decrease linearly with increasing the d_{z^2} -band center. This result suggests that, for adsorption of H atom and H_2 molecule, the binding strengths between H and 3d TM are both determined by the d_{z^2} -band center.

Due to the mainly determinant of catalytic activity for HER by H bond strength and the explicit linear relation between the H bond strength and the d_{z^2} -band center, we can use the d_{z^2} -band center as the descriptor for the active in HER. Similar to the d-band center descriptor, if the band center is too high, the H will bind strongly to the surface and have difficulty leaving from the surface; if band center is too low, the H will bind too weakly and be difficult to adsorb. High catalytic activity for HER needs a modest band center. It should be mentioned that the single atom on 2D surface is not absolute alone. It is anchored by the chemical bond on the 2D surface. The single atom here is a part of the 2D basal plane and acts as an atomic-level reactive site. Its s, p and d bands all hybridize with those of other atoms in the basal plane substrate and show continuous distribution (as shown in Figure S5). Therefore the center of energy bands can be applied to describe the reactive for this system with single-atom active sites. Furthermore, the explicit linearly relation between the band-center and the H bond strength directly confirm this feasibility.

There are both similarities and differences for the d-band center descriptor and the d_{z^2} -band center descriptor. The similarity is that the evaluation of the catalytic activity are all based on the efficiency of the adsorbate adsorption/desorption which is dominated by the bond strength of adsorbate on surface. This idea runs through our full text. The distinct difference is the reactive orbital. One is the d orbital and the other is the d_{z^2} orbital. Another difference is that they are suitable for different single-atom-anchored surface systems. The d-band center is suitable for the surface of nanoparticles system; while, the d_{z^2} -band center is valid for the surface of 2D basal

plane system. In the following, we discuss this implied difference.

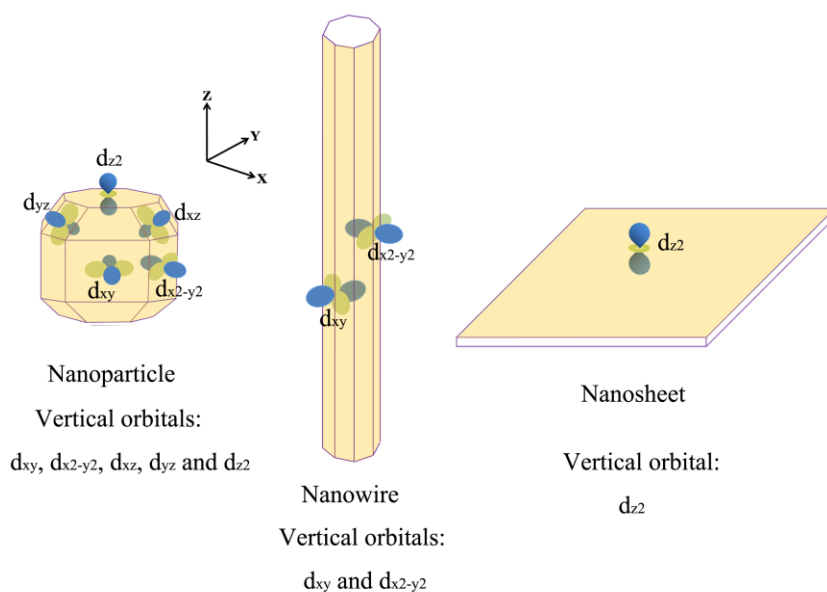


Figure 5. Vertical orbitals at various surfaces in different-dimensional systems, coordinate axis is as shown in the figure.

In catalytic reactive, the adsorbate adsorption on surface of catalysis always involve the interaction between the orbitals of catalyst active site and adsorbate. As above demonstrated, not all the orbitals of the active site participate in the interaction. For the HER of single-atom active sites, only the orbitals perpendicular to the surface can have effective interaction with H 1s orbital. In this way, the strength of the H adsorption on the surface of catalysis is mainly determined by the feature of these vertical orbitals. For a single flat surface, such as the 2D basal plane, there is only one projected d orbital perpendicular to it. If the coordinate Z axis is perpendicular to the surface, this vertical projected d orbital is the d_{z^2} orbital as shown in Figure 5. Differently, for 3D polyhedral systems, such as nanoparticles, the surface is composed of many facets with different direction. Taking the polyhedral nanoparticles with cubic crystal structure as example, the projected d orbitals d_{z^2} , d_{xy} , $d_{x^2-y^2}$, d_{xz} , and d_{yz} are perpendicular separately to five different facets with orientations (001), (110), (100), (101) and (011), respectively (as shown in Figure 5). In this case, the five projected d orbitals from the active sites on the different facets can all hybrid with H 1s orbital, and thus the band center of the each projected d orbital can describe the HER activity on their corresponding facets. The average of the band centers for the five projected d orbitals is equal to the d-band center. So the d-band center can be used to estimate the overall catalytic activity for the surface of polyhedral systems.

However, for the new system of the 2D basal plane, the vertical d orbital from the anchored active TM atom is just the d_{z^2} orbital. Therefore, the d_{z^2} -band center is only suitable for such systems.

Based on the above discussion, we can deduce that, the band center of $d_{xy}/d_{x^2-y^2}$ orbitals might be used as the descriptor for HER on the side face of the 1D nanowires or nanorods system. Because, assuming the Z axis is along the direction of the nanowires/nanorods, the vertical orbitals on the side face is the $d_{xy}/d_{x^2-y^2}$ (as shown Figure 5), which is the unique orbitals that can form bond with H atom compared to the other projected d orbitals.

4. Conclusion

In conclusion, aiming at the single-atom-anchored 2D catalysts, a new descriptor, d_{z^2} -band center for the HER activity were proposed based on the hydrogen adsorption energy. Due to the perpendicular feature to surface for the d_{z^2} orbital, for more extensive significance the descriptor can also be termed as vertical-orbital band center descriptor. Different from the traditional d-band center which can be well used to measure the catalytic activity in nanoparticles system, this descriptor is valid for the 2D basal plane system.

Acknowledgements

This work was supported by the National Natural Science Foundation of China (Grant No. 11504086), the Ten Thousand Talents Plan of Zhejiang Province of China (Grant No. 2019R52014), the Open Project of National Laboratory of Solid State Microstructures, Nanjing University (Grant No. M33010) and the School Scientific Research Project of Hangzhou Dianzi University (Grant Nos. KYS045619084, KYS045619085).

References

- [1] Gupta U and Rao C N R 2017 Hydrogen generation by water splitting using MoS_2 and other transition metal dichalcogenides *Nano Energy* **41** 49-65
- [2] Lu Q, Yu Y, Ma Q, Chen B and Zhang H 2016 2D Transition-Metal-Dichalcogenide-Nanosheet-Based Composites for Photocatalytic and Electrocatalytic Hydrogen Evolution Reactions *Advanced materials* **28** 1917-33
- [3] Lei Z, Zhan J, Tang L, Zhang Y and Wang Y 2018 Recent Development of Metallic (1T) Phase of Molybdenum Disulfide for Energy Conversion and Storage *Advanced Energy Materials* **8** 1703482
- [4] Dresselhaus M and Thomas I 2001 Alternative energy technologies *Nature* **414** 332-7
- [5] Voiry D, Yang J and Chhowalla M 2016 Recent Strategies for Improving the Catalytic Activity of 2D TMD Nanosheets Toward the Hydrogen Evolution Reaction *Advanced*

materials **28** 6197-206

- [6] Duan J, Chen S and Zhao C 2017 Ultrathin metal-organic framework array for efficient electrocatalytic water splitting *Nature communications* **8** 15341
- [7] Voiry D, Yamaguchi H, Li J, Silva R, Alves D C, Fujita T, Chen M, Asefa T, Shenoy V B and Eda G 2013 Enhanced catalytic activity in strained chemically exfoliated WS₂ nanosheets for hydrogen evolution *Nature materials* **12** 850
- [8] Anantharaj S, Ede S R, Sakthikumar K, Karthick K, Mishra S and Kundu S 2016 Recent Trends and Perspectives in Electrochemical Water Splitting with an Emphasis on Sulfide, Selenide, and Phosphide Catalysts of Fe, Co, and Ni: A Review *ACS Catalysis* **6** 8069-97
- [9] Hou Y, Qiu M, Zhang T, Zhuang X, Kim C S, Yuan C and Feng X 2017 Ternary Porous Cobalt Phosphoselenide Nanosheets: An Efficient Electrocatalyst for Electrocatalytic and Photoelectrochemical Water Splitting *Advanced materials* **29** 1701589
- [10] Zhu C, Wang A L, Xiao W, Chao D, Zhang X, Tiep N H, Chen S, Kang J, Wang X, Ding J, Wang J, Zhang H and Fan H J 2018 In Situ Grown Epitaxial Heterojunction Exhibits High-Performance Electrocatalytic Water Splitting *Advanced materials* **30** 1705516
- [11] Hu C, Zhang L and Gong J 2019 Recent progress made in the mechanism comprehension and design of electrocatalysts for alkaline water splitting *Energy and Environmental Science* **12** 2620-45
- [12] Shi Y and Zhang B 2016 Recent advances in transition metal phosphide nanomaterials: synthesis and applications in hydrogen evolution reaction *Chemical Society Reviews* **45** 1529-41
- [13] Jaramillo T F, Jorgensen K P, Bonde J, Nielsen J H, Horch S and Chorkendorff I 2007 Identification of Active Edge Sites for Electrochemical H₂ Evolution from MoS₂ Nanocatalysts *Science* **317** 100-2
- [14] Cao D, Ye K, Moses O A, Xu W, Liu D, Song P, Wu C, Wang C, Ding S, Chen S, Ge B, Jiang J and Song L 2019 Engineering the In-Plane Structure of Metallic Phase Molybdenum Disulfide via Co and O Dopants toward Efficient Alkaline Hydrogen Evolution *ACS Nano* **13** 11733-40
- [15] Wang Y, Qi K, Yu S, Jia G, Cheng Z, Zheng L, Wu Q, Bao Q, Wang Q, Zhao J, Cui X and Zheng W 2019 Revealing the Intrinsic Peroxidase-Like Catalytic Mechanism of Heterogeneous Single-Atom Co-MoS₂ *Nano-Micro Letters* **11** 1-13
- [16] Tsai C, Li H, Park S, Park J, Han H S, Norskov J K, Zheng X and Abild-Pedersen F 2017 Electrochemical generation of sulfur vacancies in the basal plane of MoS₂ for hydrogen evolution *Nature communications* **8** 15113
- [17] Wang S, Zhang D, Li B, Zhang C, Du Z, Yin H, Bi X and Yang S 2018 Ultrastable In-Plane 1T-2H MoS₂ Heterostructures for Enhanced Hydrogen Evolution Reaction *Advanced Energy Materials* **8** 1801345
- [18] Qi K, Cui X, Gu L, Yu S, Fan X, Luo M, Xu S, Li N, Zheng L, Zhang Q, Ma J, Gong Y, Lv F, Wang K, Huang H, Zhang W, Guo S, Zheng W and Liu P 2019 Single-atom cobalt array bound to distorted 1T MoS₂ with ensemble effect for hydrogen evolution catalysis *Nature communications* **10** 1-9
- [19] Lau T H M, Wu S, Kato R, Wu T-S, Kulhavý J, Mo J, Zheng J, Foord J S, Soo Y-L, Suenaga K, Darby M T and Tsang S C E 2019 Engineering Monolayer 1T-MoS₂ into a Bifunctional Electrocatalyst via Sonochemical Doping of Isolated Transition Metal Atoms *ACS Catalysis* **9**

- [20] Meng K, Wen S, Liu L, Jia Z, Wang Y, Shao Z and Qi T 2019 Vertically Grown MoS₂ Nanoplates on VN with an Enlarged Surface Area as an Efficient and Stable Electrocatalyst for HER *ACS Applied Energy Materials* **2** 2854-61
- [21] Ouyang Y, Ling C, Chen Q, Wang Z, Shi L and Wang J 2016 Activating Inert Basal Planes of MoS₂ for Hydrogen Evolution Reaction through the Formation of Different Intrinsic Defects *Chemistry of Materials* **28** 4390-6
- [22] Luo Z, Ouyang Y, Zhang H, Xiao M, Ge J, Jiang Z, Wang J, Tang D, Cao X, Liu C and Xing W 2018 Chemically activating MoS₂ via spontaneous atomic palladium interfacial doping towards efficient hydrogen evolution *Nature communications* **9** 2120
- [23] Li H, Tsai C, Koh A L, Cai L, Contryman A W, Fragapane A H, Zhao J, Han H S, Manoharan H C and Abildpedersen F 2016 Activating and optimizing MoS₂ basal planes for hydrogen evolution through the formation of strained sulphur vacancies *Nature Materials* **15** 48-53
- [24] Conway B and Tilak B 2002 Interfacial processes involving electrocatalytic evolution and oxidation of H₂, and the role of chemisorbed H *Electrochimica Acta* **47** 3571-94
- [25] Hinnemann B, Moses P G, Bonde J, Jørgensen K P, Nielsen J H, Horch S, Chorkendorff I and Nørskov J K 2005 Biomimetic hydrogen evolution: MoS₂ nanoparticles as catalyst for hydrogen evolution *Journal of the American Chemical Society* **127** 5308-9
- [26] Lau T H, Lu X, Kulhavy J, Wu S, Lu L, Wu T-S, Kato R, Foord J S, Soo Y-L and Suenaga K 2018 Transition metal atom doping of the basal plane of MoS₂ monolayer nanosheets for electrochemical hydrogen evolution *Chemical science* **9** 4769-76
- [27] Luo Y, Zhang S, Pan H, Xiao S, Guo Z, Tang L, Khan U, Ding B-F, Li M, Cai Z, Zhao Y, Lv W, Feng Q, Zou X, Lin J, Cheng H-M and Liu B 2019 Unsaturated Single Atoms on Monolayer Transition Metal Dichalcogenides for Ultrafast Hydrogen Evolution *ACS Nano* **14** 767-76
- [28] Wang Q, Zhao Z L, Dong S, He D, Lawrence M J, Han S, Cai C, Xiang S, Rodriguez P and Xiang B 2018 Design of active nickel single-atom decorated MoS₂ as a pH-universal catalyst for hydrogen evolution reaction *Nano Energy* **53** 458-67
- [29] Mo J, Wu S, Lau T H M, Kato R, Suenaga K, Wu T S, Soo Y L, Foord J S and Tsang S C E 2020 Transition metal atom-doped monolayer MoS₂ in a proton-exchange membrane electrolyzer *Materials Today Advances* **6** 100020
- [30] Qiao W, Xu W, Xu X, Wu L, Yan S and Wang D 2020 Construction of Active Orbital via Single-Atom Cobalt Anchoring on the Surface of 1T-MoS₂ Basal Plane toward Efficient Hydrogen Evolution *ACS Applied Energy Materials* **3** 2315-22
- [31] Nørskov J K, Bligaard T, Logadottir A, Kitchin J R, Chen J G, Pandelov S and Stimming U 2005 Trends in the Exchange Current for Hydrogen Evolution *Journal of The Electrochemical Society* **152** J23
- [32] Li F, Han G-F, Noh H-J, Jeon J-P, Ahmad I, Chen S, Yang C, Bu Y, Fu Z, Lu Y and Baek J-B 2019 Balancing hydrogen adsorption/desorption by orbital modulation for efficient hydrogen evolution catalysis *Nature communications* **10** 1-7
- [33] Hinnemann B, Moses P G, Bonde J, Jørgensen K P, Nielsen J H, Horch S, Chorkendorff I and Nørskov J K 2005 Biomimetic Hydrogen Evolution: MoS₂ Nanoparticles as Catalyst for Hydrogen Evolution *Journal of the American Chemical Society* **127** 5308-9
- [34] Nørskov J K, Bligaard T, Rossmeisl J and Christensen C H 2009 Towards the computational

- design of solid catalysts *Nature Chemistry* **1** 37-46
- [35] Norskov J K, Abild-Pedersen F, Studt F and Bligaard T 2011 Density functional theory in surface chemistry and catalysis *Proceedings of the National Academy of Sciences of the United States of America* **108** 937-43
- [36] Kitchin J R, Norskov J K, Barteau M A and Chen J G 2004 Role of strain and ligand effects in the modification of the electronic and chemical properties of bimetallic surfaces *Physical review letters* **93** 156801
- [37] Kibler L A, El-Aziz A M, Hoyer R and Kolb D M 2005 Tuning reaction rates by lateral strain in a palladium monolayer *Angewandte Chemie* **44** 2080-4
- [38] Ruban A, Hammer B, Stoltze P, Skriver H L and Nørskov J K 1997 Surface electronic structure and reactivity of transition and noble metals *Journal of Molecular Catalysis A: Chemical* **115** 421-9
- [39] Hammer B and Nørskov J 1995 Electronic factors determining the reactivity of metal surfaces *Surface Science* **343** 211-20
- [40] Mavrikakis M, Hammer B and Nørskov J K 1998 Effect of strain on the reactivity of metal surfaces *Physical review letters* **81** 2819
- [41] Hwang J, Noh S H and Han B 2019 Design of active bifunctional electrocatalysts using single atom doped transition metal dichalcogenides *Applied Surface Science* **471** 545-52
- [42] Fu W, Wang Y, Tian W, Zhang H, Li J, Wang S and Wang Y 2020 Non-metal single-phosphorus-atom catalysis of hydrogen evolution *Angewandte Chemie* **132** 23999-4007
- [43] Fang S, Zhu X, Liu X, Gu J, Liu W, Wang D, Zhang W, Lin Y, Lu J and Wei S 2020 Uncovering near-free platinum single-atom dynamics during electrochemical hydrogen evolution reaction *Nature communications* **11** 1-8
- [44] Liu G, Robertson A W, Li M M, Kuo W C H, Darby M T, Muhieddine M H, Lin Y, Suenaga K, Stamatakis M and Warner J H 2017 MoS₂ monolayer catalyst doped with isolated Co atoms for the hydrodeoxygenation reaction *Nature Chemistry* **9** 810-6
- [45] Odkhuu D 2016 Giant perpendicular magnetic anisotropy of an individual atom on two-dimensional transition metal dichalcogenides *Physical Review B* **94** 060403
- [46] Li J, Chen S, Quan F, Zhan G, Jia F, Ai Z and Zhang L 2020 Accelerated dinitrogen electroreduction to ammonia via interfacial polarization triggered by single-atom protrusions *Chem* **6** 885-901

Supporting Information

Vertical-orbital band center as an activity descriptor for hydrogen evolution reaction on single-atom-anchored 2D catalysts

Wen Qiao¹, Shiming Yan^{1*}, Deyou Jin¹, Xiaoyong Xu², Wenbo Mi³, Dunhui Wang¹

1 School of Electronics and Information, Hangzhou Dianzi University, Hangzhou 310018, China

2 School of Physics Science and Technology, Yangzhou University, Yangzhou, 225002, China

3 Tianjin Key Laboratory of Low Dimensional Materials Physics and Preparation Technology,

School of Science, Tianjin University, Tianjin 300354, China

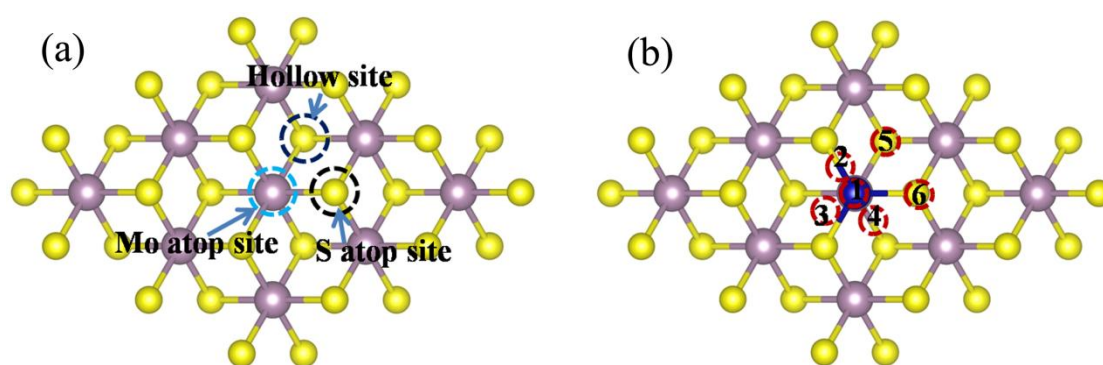


Figure S1. Schematic of possible TM anchoring site. (b) Initial H adsorbed position for geometric optimizing.

Table S1. Binding energy for series TMs occupying on different surface site.

	Binding Energy (eV)					
	V	Cr	Mn	Fe	Co	Ni
Mo atop site	-3.37	-1.46	-1.37	-2.94	-4.09	-3.81
S atop site	0.04	2.02	1.99	0.04	-1.46	-2.04
Hollow site	-3.30	-1.40	-1.23	-2.57	-3.56	-3.22

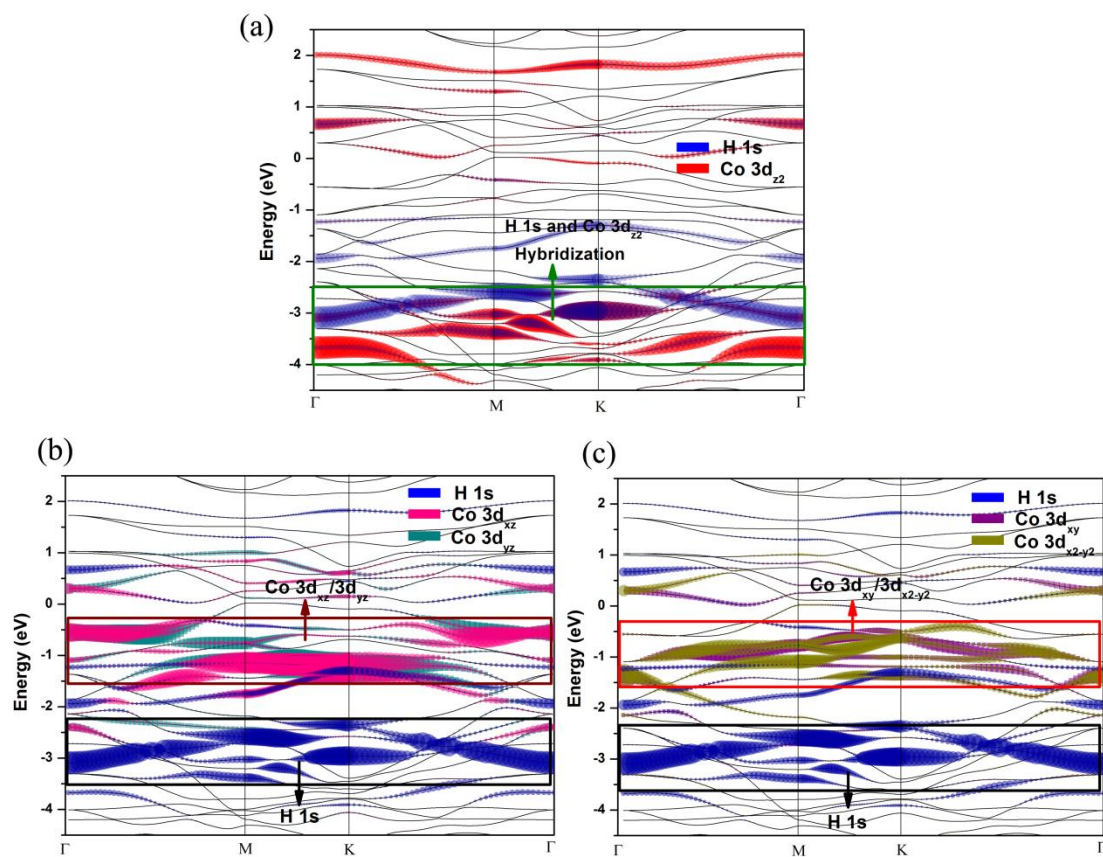


Figure S2. The calculated orbital-resolved bands structure for the 1T-MoS₂-Co with H adsorption.

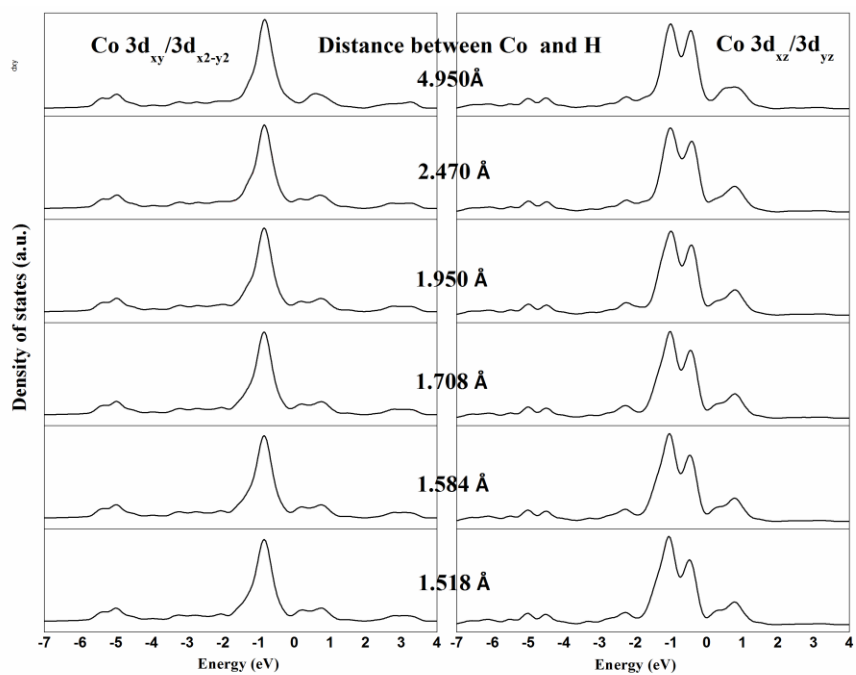


Figure S3. PDOS of Co $3d_{xy}/3d_{x^2-y^2}$ and $3d_{xz}/3d_{yz}$ orbitals at different the distance of Co-H.

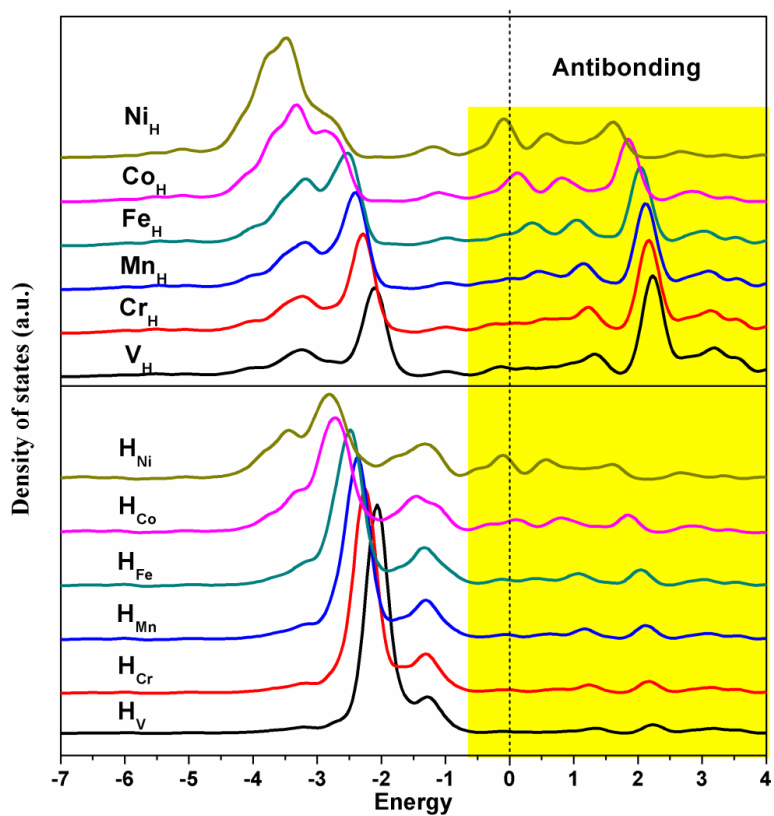


Figure S4. PDOSs of the TMs d_{22} orbitals and the corresponding H 1s orbitals in series TMs anchoring on 1T-MoS₂ with H adsorption.

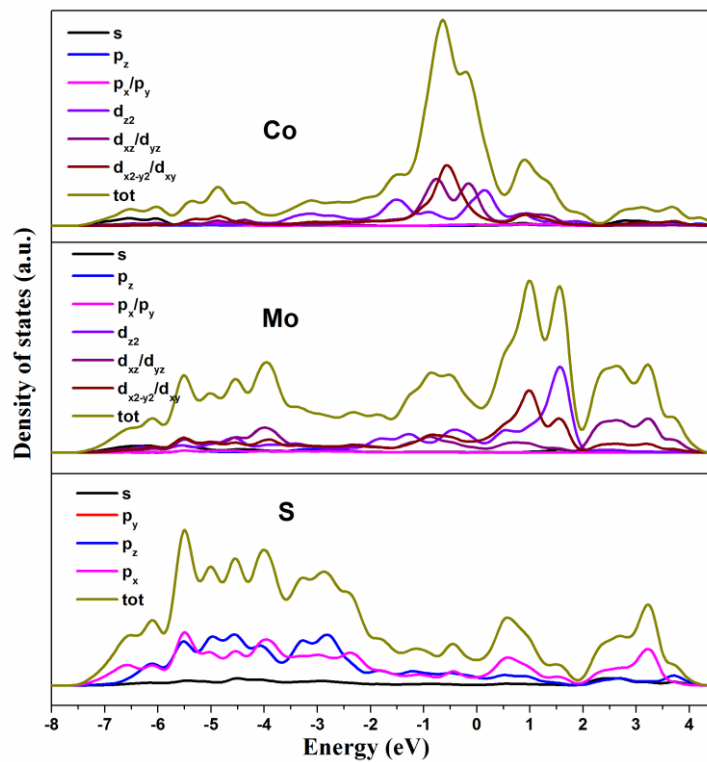


Figure S5. DOSs and PDOSs of the different orbitals for Co, Mo and S atoms in 1T-MoS₂-Co.

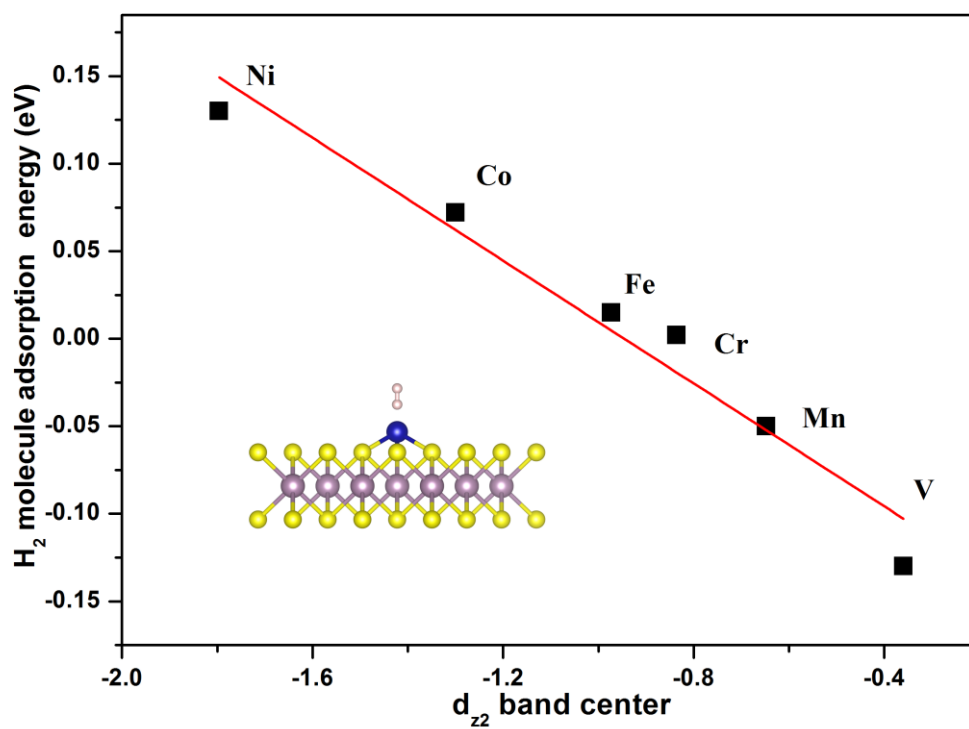


Figure S6. Dependence of the d_{z²}-band center on H₂ molecule adsorption energy for the series 3d TMs anchored on basal planes of 1T-MoS₂.

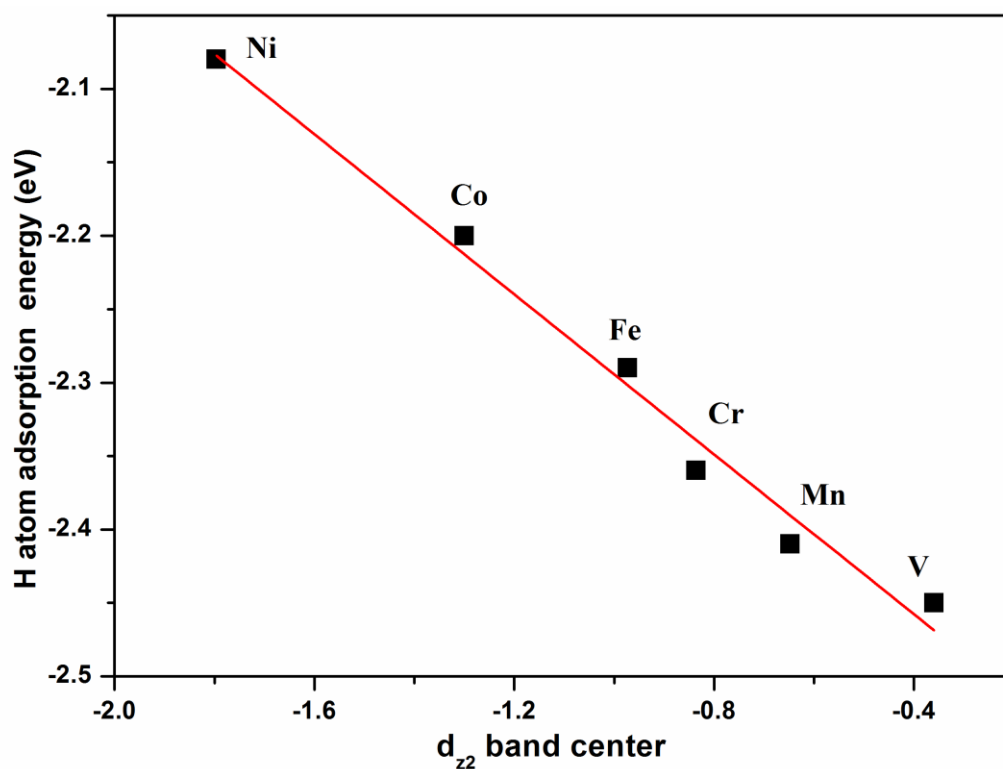


Figure S7. Dependence of d₂₂-band center on H atom adsorption energy for the series 3d TMs anchored on basal planes of 1T-MoS₂. Different from H adsorption energy, the H atom adsorption energy is defined as $\Delta E_H = E_{2D-BP-SA+H} - E_{2D-BP-SA} - E_H$.